



Investigate the Impact of Ni-Doped ZNO NPS on The Antibacterial Activity and Degradation Rate of Polyacrylic Acid-Modified Starch Nanocomposite

Sajjani, Research Scholar, Department of Chemistry, Baba Mastnath University, Rohtak sajjanirathee13@gmail.com

Pallavi Bhardwaj, Associate Professor, Department of Chemistry, Baba Mastnath University, Rohtak,

pallavi198277@gmail.com

Pankaj Kumar, GM, Research and Development, RTF Nashik, Maharashtra, pnkjiitb@gmail.com

Ritu Nandal, Assistant professor, Pt. Neki Ram Sharma Govt College Rohtak, ritu9051@gmail.com

(Received: 15 November 2023

Revised: 23 December

Accepted: 27 January)

KEYWORDS

Polyacrylic,
Nanocomposites,
Acid-Modified
starch Nanoparticle
incorporation.

ABSTRACT

The current work examines the effects of adding nickel-doped zinc oxide nanoparticles (Ni-Doped ZnO NPs) to materials that are polyacrylic acid-modified starch nanocomposite (PAA-Starch NC) on their antibacterial activity and rate of degradation. Although PAA-Starch is a biodegradable polymer with excellent water absorption & film-forming capabilities, it is not very efficient against bacteria and degrades slowly. In the production of PAA starch, ammonium persulfate was used as a free radical initiator, in conjunction with the biodegradable nonionic surfactant Dec oxyethylene n-decyl ether, commonly referred to as Lutensol-XL-100. In order to control the rate at which the composite plastic degrades, a nanocomposite (NC) was synthesized through the combination of Ni-Doped ZnO NPs with an optimized thin film of starch-based plastic. Several techniques, such as FTIR, TGA, DSC, & SEM, were used to characterize the NC. By increasing the composite film's heat resistance and inhibiting bacterial growth, ZnO@Ni NPs gave it antibacterial properties. After 60 days in soil, biodegradation of starch-grafted PAA was 23.21%, compared to 16.19% for its NC. The results of the antimicrobial tests on the composite film were outstanding.

INTRODUCTION

Growing interest is being paid to the creation of bio-based goods and cutting-edge production techniques that can result in high-tech materials that are ecologically benign and biodegradable (Tran et al., 2019; Magni et al., 2020). As the circular bioeconomy continues to grow, goods based on NC technology are emerging as the next generation of materials. Renewable NC-based biodegradable polymers, polyhydroxy alkenoates, corn-derived plastic, & cellulosic plastic are all candidates for future biopolymers, according to previous research (Saba et al., 2019; Shen et al., 2020; Chen and Yan, 2020; Saikia et al., 2019; Iqbal et al., 2017; Shafqat et al., 2020; Briassoulis et al., 2021). Assembling NCs for many uses requires only the incorporation of NPs into biodegradable polymers (Zare et al., 2019, Bahadur et al., 2018; Waqas et al., 2017; Anwer et al., 2018).

NC materials, which combine the advantageous properties of NPs with the versatility of polymers, have emerged as a pivotal area of research in recent years. These versatile materials have a variety of applications, including drug delivery systems, environmental remediation, and antimicrobial coatings. This investigation into a particular NC system aims to cast light on how the incorporations of Ni-Doped ZnO NPs into a PAA- Starch NC affects its antibacterial activity degradation rate.

PAA-Modified Starch is a biocompatible and biodegradable polymer. It has garnered attention for its suitability in various applications due to its exceptional characteristics, such as high-water absorbency, film-forming ability, and low toxicity. However, like many biopolymers, PAA-Starch has limitations when it comes to antibacterial performance and degradation rate. These



limitations have driven researchers to explore innovative strategies to overcome these challenges, and one promising avenue is the incorporation of NPs.

Given their unique characteristics and a better comprehension of the underlying processes that occur at the nanoscale, NC materials are currently becoming more and more popular. The purpose of blending is to combine all of the polymers in the mix to get the desired characteristics. Metal NPs have the potential to serve as additives in both organic and inorganic composites, thereby enhancing the structural, optical, & electrical properties of materials such as sodium alginate (NaAlg) and PEO. Materials containing NPs are used to create polymeric NCs with a significant surface area (Hussein et al., 2020). Chemical, electrical, and photocopier industries all employ Ni/ZnO NPs metal NPs in a range of industrial applications (Yaacob et al., 2014). Ni/ZnO NPs can be applied to food packaging, antimicrobial coatings, medical equipment, & nutritional supplements. The creation of polymer mix systems has been aided by the use of NaAlg, a biodegradable, nontoxic natural polymer, for PEO to contain more amorphous phases. Phase separation in the generated films is also less frequent when NaAlg is used. Because of its OH groups, NaAlg can form H-bonds with other polymers, such as PEO. Because of its special characteristics, NaAlg is employed in several industries, including as paper & pharmaceutical, electronics, and food packaging (Lopez et al., 2015). Both crystalline and amorphous forms of the semicrystalline polymer PEO have been discovered (Jang et al., 2003). PEO is renowned for its outstanding non-ionic, high viscosity, heat-formative, water-soluble, and thermal and chemical stability (Angot et al., 2000).

The focus on Ni-Doped ZnO NPs is strategic. ZnO NPs have gained recognition for their remarkable antibacterial properties, particularly when exposed to ultraviolet (UV) light. Under UV irradiation, ZnO NPs generate ROS, such as O₂ & OH radicals, which exhibit potent antibacterial effects. By introducing nickel doping into ZnO NPs, their properties can be finely tuned and enhanced, potentially leading to an improvement in antibacterial performance. This study aims to comprehensively investigate how the presence of these engineered NPs influences the antibacterial activity of PAA-Starch NCs.

Eco-friendly biodegradable polymer composites have

historically had a strong reliance on plant resources (Jadhav et al., 2019; Kabir et al., 2020). Starches have been recognized by several scientists for adaptation to modern demands since they are the most plentiful, least priced, & broadly available of these natural resources (Shabana et al., 2019; Sintim et al., 2020). The two primary types of starch, amylose & amylopectin, are abundant in corn, wheat, and rice. The four methods for altering polymers are blending, derivatization, curing, & grafting (Gurunathan et al., 2015).

This research extends beyond the realm of antibacterial properties. The degradation behavior of the resulting NC is a critical aspect to consider. In some applications, such as agricultural films or drug delivery systems, controlled degradation is a desirable feature. The introduction of NPs, including Ni-Doped ZnO NPs, can alter the degradation profile of the NC. This includes factors like the rate of degradation, the environmental conditions required for degradation, and the resulting byproducts. Understanding these effects is vital for tailoring the material's longevity, sustainability, and environmental impact.

(Alghamdi et al., 2022) developed a film using NaC₆H₇O₆, polyethylene oxide (PEO), & Ni & ZnO NPs as antimicrobials. Nanohybrid Ni/ZnO NPs with weight percentages of 0%, 5%, 10%, 15%, & 20% were created using the sol-gel method. The enhanced NaAlg/PEO-Ni/ZnO NC has a 47% reduction in crystallinity. Through FTIR analysis, interactions b/w Ni/ZnO & NaAlg/PEO NP have been discovered. They examined the biodegradable NCs' mechanical, electrical, & dielectric properties. The NCs' AC conductivity & dielectric characteristics were improved by using additional Ni/ZnO NPs. Mechanical properties of the NC were improved by adding Ni/ZnO NPs. The principal research foci were *E. coli* and *S. aureus*, two Gram-positive (GP) and Gram-negative (GN) microorganisms. Greater antibacterial effectiveness was seen against yeast, fungus, *S. aureus*, and *E. coli* when Ni/ZnO NPs & NaAlg/PEO were coupled. As the Ni/ZnO NPs content rose, The NC film's water solubility dropped from 65.5% to 9.81%. (Anugrahwidya et al., 2022) observed that ZnO NCs considerably improved the crystallinity & tensile strength of bioplastics. The strongest ZnO- bioplastics



have a 13% concentration, and both regular soil & seawater may completely break them down in less than 30 days. The strongest ZnO- bioplastics have a 13% concentration, and both regular soil and seawater may completely break them down in less than 30 days. Microbiological analysis of packaged samples revealed that the shelf life of sliced bread in PZ & PK has been extended from 10 to 30 days. All of the active coatings inhibited mold growth in the bread for 30 days, but the coatings containing 10, 13, & 16% ZnO NCs demonstrated the greatest improvement in antimicrobial properties, with no fungal growth observed. This research depicts the potential of ZnO NCs as a green additive to starch & starch/chitosan-based bioplastics for application in increasing the food in packaged form's shelflife.

(Saemi et al., 2021) synthesized ZnO NPs from a walnut leaf extract using 5-25 g of leaves, 30-90 minutes of reaction time, & a 60°C heater & stirrer. By using FTIR spectroscopy and GC, 29 bioactive compounds and six major functional groups were found in the walnut leaf extract. Response surface methodologies were used to enhance the antioxidant & antibacterial inhibitory activities of powdered ZnO NPs. The model for the powdered ZnO NPs was built using two fake variables. With 15.51 g of walnut leaf extract's dry powder & a reaction time of 60 min, the ZnO NPs with the highest antibacterial & antioxidant activity against.

E. coli were those that were generated. Particle sizes of ZnO NPs range from 15 to 40 nm were created from crystals with triangular nanoprisms to nearly spherical form, according to XRD investigations and SEM photos. Researchers were able to create a biodegradable film that was very effective at preventing both GP (*S. aureus*) and GN (*E. coli*) bacterial growth.

(Lian et al., 2021) investigated how ZnO-NPs affected physical and chemical characteristics, antibacterial activity, & cytocompatibility. In this study, the plasticizers chitosan (CS) & ZnO-NPs were utilized. Since L-malic acid has a less strong smell than acetic acid, it was used to make a solution of chitosan. In terms of physicochemical parameters, the best composite films had a mass ratio of CS/ST of 1:1, 6% (w/w) ZnO-NPs, and a TS value of 19.64±0.75 MPa. The *S. aureus* inhibition zones for the

composite films containing ZnO-NPs after 0, 7, & 14 days of sustained release were 29.36±2.40 mm, 24.90±0.40 mm, & 22.00±0.34 mm, respectively ($p<0.05$). ZnO-NPs-containing composite films were demonstrated to be cytocompatibility by MC3T3-E1 cells' ability to survive on their surfaces (95.633.17%; $p<0.05$).

The size, shape, & antibacterial activity of ZnO NPs made from leftover pineapple peels were investigated by (Hassan et al., 2020). ZnO NPs' size & shape fluctuate when the synthesis temperature changes, as shown by micrographs collected at 28 and 60 C. Both spherical and rod- shaped NPs with diameters between 8 and 45 nm were detected in the non-heated condition (28 °C), whereas only rod-shaped NPs with sizes between 73 and 123 nm were discovered in the heated (60 °C) state. ZnO and starch NC films at 1, 3, & 5 wt. %. The ZnO NPs were created using a technique known as film casting. The disc diffusion method was employed to see if the films inhibited the development of GP and GN bacteria. According to the findings, the inhibitory zone against GP bacteria, particularly *Bacillus subtilis*, increased as ZnO NP content in the film grew from 1 to 5 wt%.

(Hu et al., 2019) investigated composite films made from antibacterial NPs & a modified starch matrix. By weight, the sol-gel synthesized ZnO- chitosan NPs had a 57.3% ZnO content & a hexagonal phase. With an absorbance peak at about 364 nm, NPs had an average size of 25 nm. The distribution of NPs below 3.0 weight percent was found to be homogeneous throughout the starch matrix. As the number of NPs in the films increased, both the tensile strength & the water vapor permeability increased from 4.11 to 12.79 MPa ($p<0.05$) and dramatically dropped from 51.0% to 43.7%, respectively. At increasing levels of 4.0–5.0 wt%, films showed improved water vapor permeability and nanoparticle agglomeration ($p<0.05$). The growth of Gram-positive *Staphylococcus aureus* was found to be more effectively inhibited by starch-based films compared to Gram-negative *Escherichia coli*. Furthermore, this inhibitory effect was observed to be positively associated with the concentration of NPs loaded onto the films.



MATERIALS AND METHODS

Materials

The reagents and chemicals were all purchased and utilised exactly as they were. We purchased acrylic acid, acrylonitrile, methacrylate, starch, ammonium persulfate, zinc (NO₃)₂·6H₂O, nickel chloride, sodium hydroxide, and LutensolXL-100 from local merchants.

Synthesis of ZnO and Ni-doped ZnO NPs

The method for preparing ZnO NPs was derived from published papers (Mondal et al., 2020). NPs of ZnO were produced via bottom-up chemical coprecipitation. A 100 mL solution of Zn (NO₃)₂·6H₂O with a concentration of 0.5 M was promptly produced in deionized water. Under ideal conditions, the solution was placed in a flask with a round bottom, heated to 60 °C, and 40 emitted to reflux for six hours.

White precipitates formed after the reaction was complete and the mix was cooled to room temp. Multiple washing in DI water/ethanol and overnight drying at 80°C were used to remove the precipitates. The ZnO NPs were subjected to a calcination technique in a muffle furnace, where they were heated to 580°C at a rate of 5°C per minute for 4 hours

Synthesis of Ni-doped ZnO NPs

Bottom-up chemical co-precipitation was used to create Ni-doped ZnO NPs. To recap, in DI water, 100 mL of a 0.5 M Zn (NO₃)₂·6H₂O solution containing 2% (w) NiCl was generated, and the pH was maintained by adding a dropwise amount of a 2 M NaOH solution. The solution was then put in a flask with a circular bottom and exposed to ideal conditions, including heating & refluxing at 60±1°C for 6 hours.

Following the formation of precipitates, the solution was subsequently cooled to attain ambient temp. The precipitates were washed numerous times in a solution of DI water and ethanol after being dried in an oven at 80 °C for 12 hours. Finally, a muffle furnace was used to calcine the Ni-doped ZnO NPs (2 wt%) for 4 hours at 580°C (5C/minutes).

Preparation of Thin Film

One gramme of starch with 25 ml distilled water and digested by heating it over a Bunsen flame. The complete components were combined in a reaction kettle with three necks and a magnetic stirrer. It was the response kettle put in an 80°C water bath once a clear solution had been

obtained. After waiting 10 minutes, we emulsified the mixture by adding 10– 12 drops of Lutensol XL–100. After 10 minutes of thorough mixing, 0.150 g of K₂S₂O₈ was introduced as an initiator. Then, at a rate of one millilitre per minute, three millilitres of acrylic acid were added. We heated the mixture to 80°C after adding all of the monomers and kept it there for 1.5 hours to finish the reaction using 0.02 g of Ni-doped ZnO NPs. The final step was bringing the product to room temperature. The entire chemical route for converting starch & acrylic acid into starch-g-PAA is shown in Figure. 1.

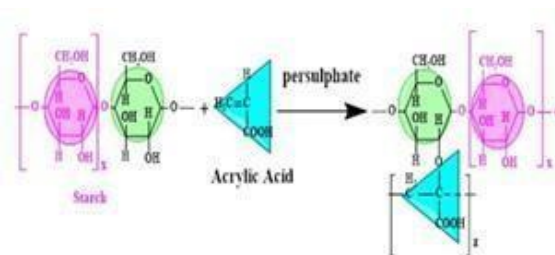


Fig 1. Starch-g-PAA forms from acrylic acid and starch.

Characterization methods

ThermoScientific Nicolet6700 FTIR

spectrophotometer was employed to get the FTIR spectra of the NC & starch. Differential scanning calorimetry (DSC) & thermogravimetric analysis. (TGA) were used to observe the product's thermal change. The product's surface morphology and biodegradability were investigated using a TESCAN Vega LMU variable pressure SEM.

RESULT AND DISCUSSION

Physicochemical properties of starch-g-PAA

SEM analysis was utilized to examine the surface morphology of polymeric starch that had been fused with transition metal Ni & metal oxide ZnO. The granular characteristics visible in SEM images of pure starch were disturbed during the gelation process. The amount of grafting with the starch backbone had an impact on the form of the grafted polymer (Fig. 2).

The created NCs clumped together, as shown by the SEM images, to create a porous structure. At low monomer concentrations, there were a few minor morphological changes (Fig. 2a & b), but the structure offered little



explanation. SEM images at a greater monomer concentration (Fig. 2c & d) provided an explanation for the porosity structure & demonstrated increased grafting in this region. As can be seen in Fig. 2d, Ni-doped ZnO NPs were uniformly distributed across pure starch with just minimal aggregations. The aggregation of the small particles was also shown by these gaps (Fig. 2d). With Ni-doped ZnO NPs, high-quality hollow structures can be produced. It has been demonstrated that the granular topologies of starch are essential.

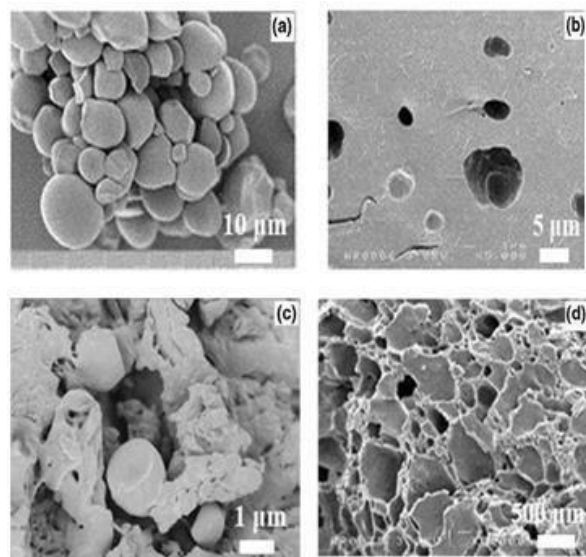


Fig 2. SEM images of the composite thin film: (a), (b), (c), and (d) at different magnifications

The O-H bond's elongation is indicated by a hump at 3000–3500 cm^{-1} (Inverse Centimeter) in FTIR starch spectrum (Fig. 3a). Stretching of the 46 C-H bonds was visible as a peak at 2930 cm^{-1} . The starch's glucose ring structure & glycosidic bond can both be seen at 1070 cm^{-1} (ether linkage). As observed in Fig. 3b, significant peaks can be found in the NC spectra. The peak at 1440 cm^{-1} in the NC is an illustration of C=C stretching. The presence of a signal at 1710 cm^{-1} indicates that sample includes a carbonyl group. The R – COO – R' group in sample is represented by a peak at 1150-1180 cm^{-1} , and glycosidic bond is showed by a peak at 1080 cm^{-1} .

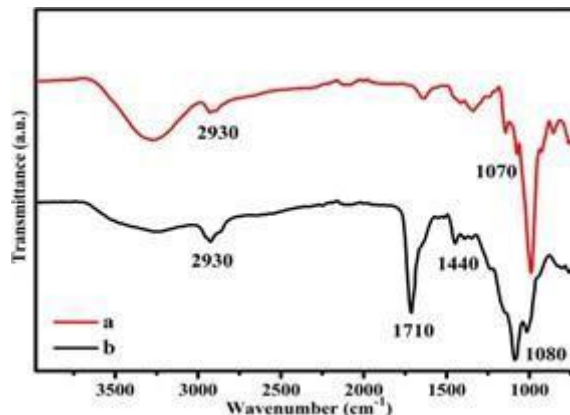


Fig 3. FTIR spectra of: (a) starch, and (b) the NC

X-ray photoelectron spectroscopy (XPS) investigation of the metal components of the starch NC has also been performed (Fig. 4), which provides details on their chemical states and surface compositional distribution. According to the ZnO literature (Shen et al., 2020; Iqbal and Iqbal, 2013) the typical peaks of Zn 2p in ZnO@Ni NPs' high-resolution XPS spectra are found at energies of 1021.7 eV (Zn 2p_{3/2}) & 1044.7 eV (Zn 2p_{1/2}). In the high-resolution O 1s spectra of the NC (Fig. 4b), Zn-O and C-O peaks with binding energies of 530.6 & 531.3 eV are both detectable. The ZnO@Ni of Ni²⁺ was ascribed to two peaks in the high-resolution Ni 2p spectra of the starch NC (Fig. 4c) that have binding energies of 853.7 & 871.1 eV. Studies on Ni-doped ZnO materials (Bahariqushchi et al., 2020) are consistent with this. ZnO@Ni interaction at the nanoscale was confirmed by XPS measurements. According to this, ZnO & Ni are in intimate touch. The C 1s spectra have three secondary peaks at 286.3, 287.0, and 289.1 eV for the C-OH, C=O, and COOH groups, and a major peak at 285.1 eV for the C-C/C-H groups. Keep an eye out for the peak at 287.7 eV; it's likely the result of numerous stacked carbon bonds like C-O and O-glycosidic. The XPS results support the final starch NC's inclusion of Ni-doped ZnO NPs as a result.

As can be observed in Figure 5, the thermal behaviour of NCs is faithfully represented by the TGA thermogram. Up to 100 °C of drying was used to remove the water from the polymer. The polymer was shown to be losing weight steadily up to 230 °C;



however, at 430 °C, the weight loss accelerated, & at 360 °C, a minor bend was observed. At 700 °C, the NC was finally destroyed. The transitions' permanence is confirmed by DSC line analysis. In the middle of the line, there were two observable bumps.

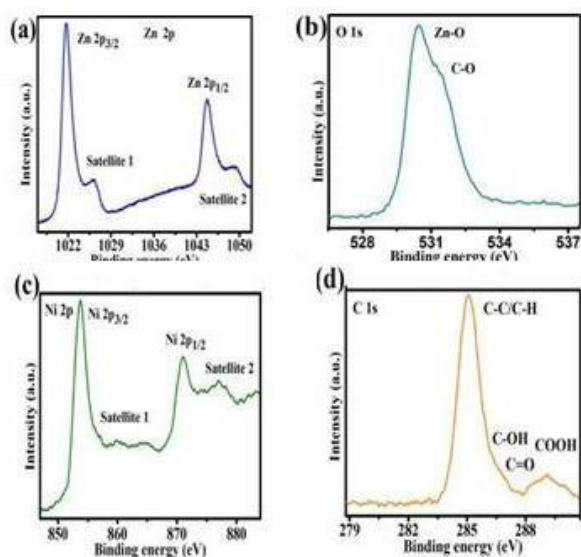


Fig 4. High-resolution XPS spectra of the starch NC:
(a) Zn 2p, (b) O 1s, (c) Ni 2p, and (d) C 1s

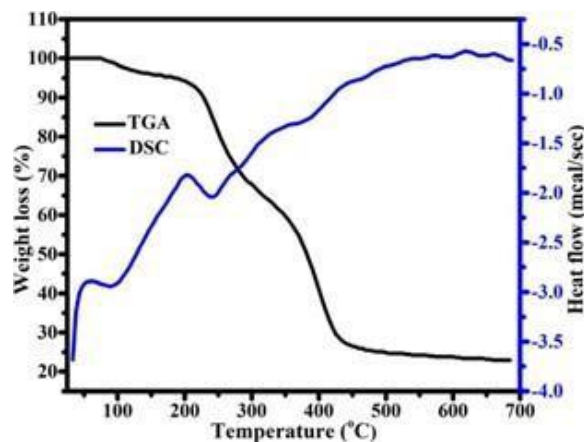


Fig 5. TGA and DSC for starch NC

Polymer and NC Weight Loss Percentage

Preparation of samples for Biodegradability

After making sample films, they were chopped into consistent dimensions and weight, with each strip being 1.5 cm wide, 8 cm long, having a thickness of 0.1 cm, & weighing nearly 1 g. Before burying them as

soil samples, we weighed the contents of two similar pots filled with soil. The weight loss of the containers was calculated after 30 days of storage in aluminum foil at room temperature.

Comparison of Biodegradability of the polymer and its NC

In comparison to the basic grafted polymer's (H-1) weight loss percentage, the NC polymer's (H-2) weight loss percentage was relatively low, according to the biodegradation data (Fig. 6). The polymer lost such a small percentage of its weight, which was explained by the outcomes that showed the NPs could resist microbial attack. NC polymer was not good moisture absorbent & did not break down quickly. For this reason, you ought to employ them for packaging & in the medical field (Table 1).

Table 1. Percentage weight loss of polymer and its NC.

Time duration of the sample	% Weight loss (without NC)	% Weight loss (with NC)
The initial weight of the sample (g)	1.13	1.06
After 10 days	-1.79	-1.89
After 20 days	2.68	3.80
After 30 days	5.37	2.86
After 40 days	8.94	9.51
After 50 days	12.50	10.50
After 60 days	23.22	16.20

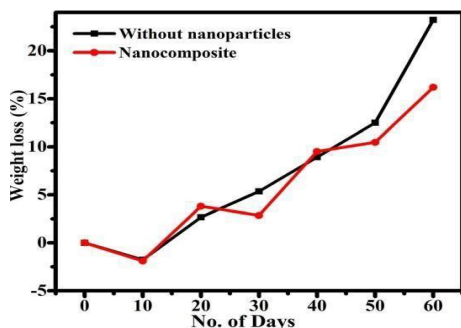


Fig 6. Biodegradability of polymer and NC.

Antibacterial study

Table 2 displays the findings of an experiment examining the antibacterial properties of polymer NCs against E. coli. Table 2 displays the high antibacterial activity of PN (0.5 mg mL⁻¹) against the bacterial isolates. The inclusion of Ni-doped ZnO and the increased surface area are responsible for the polymer composites' improved antibacterial activity. The interaction between different bacterial species and the elements of the NC polymer constitutes the putative antibacterial mechanism.

Table 2. POLYMER NC antibacterial performance

Antibacterial agent	Escherichia coli
50L	mm
Negative control	00
Positive control	18
ZnO	07
Ni-ZnO	13
2% Ni-ZnO/starch-AA NC	06
Other works	6-24

CONCLUSION

In this study, the research into how Ni-Doped ZnO NPs influence PAA Starch destruction and antibacterial potential candidate for applications in antimicrobial coatings and packaging materials. Furthermore, the introduction of these NPs has also contributed to an improved degradation rate of the NC, emphasizing its potential as an environmentally friendly material. This

research underscores the potential of nanotechnology in advancing the functional properties of biodegradable polymers for various industrial and biomedical applications, while also emphasizing the importance of further exploration into the long-term environmental implications of such materials.

activity NC has yielded positive results. The incorporation of Ni-Doped ZnO NPs has exhibited enhanced antibacterial properties, making the NC a

REFERENCES

1. Abdallah, W., Mirzadeh, A., Tan, V. and Kamal, M.R., 2018. Influence of nanoparticle pretreatment on the thermal, rheological and mechanical properties of PLA-PBSA nanocomposites incorporating cellulose nanocrystals or montmorillonite. *Nanomaterials*, 9(1): p.29.
2. Alghamdi, H. M., Abutalib, M. M., Mannaa, M. A., Nur, O., Abdelrazek, E. M., & Rajeh, A., 2022. and environmentally safe polymer nanocomposites
3. Angot, S., Taton, D., & Gnanou, Y., 2000. Amphiphilic stars and dendrimer-like architectures based on poly (ethylene oxide) and polystyrene. *Macromolecules*, 33(15): pp.5418-5426.
4. Anugrahwidya, R., Armynah, B., & Tahir, D., 2022. Composites bioplastic film for various concentration of zinc oxide (ZnO) nanocrystals towards physical properties for high biodegradability in soil and seawater. *Journal of Polymers and the Environment*, 30(6): pp.2589-2601.
5. Anwer, S., Bharath, G., Iqbal, S., Qian, H., Masood, T., Liao, K., Cantwell, W.J., Zhang, J. and Zheng, L., 2018. Synthesis of edge-site selectively deposited Au nanocrystals on TiO₂ nanosheets: an efficient heterogeneous catalyst with enhanced visible-light photoactivity. *Electrochimica Acta*, 283: pp.1095-1104.



6. Bahadur, A., Iqbal, S., Shoaib, M. and Saeed, A., 2018. Electrochemical study of specially designed graphene-Fe₃O₄-polyaniline nanocomposite as a high-performance anode for lithium-ion battery. *Dalton Transactions*, 47(42): pp.15031-15037.
7. Bahariqushchi, R., Cosentino, S., Scuderi, M., Dumons, E., Tran-Huu-Hue, L.P., Strano, V., Grandjean, D., Lievens, P., Poulin-Vittrant, G., Spinella, C. and Terrasi, A., 2020. Free carrier enhanced depletion in ZnO nanorods decorated with bimetallic AuPt nanoclusters. *Nanoscale*, 12(37): pp.19213-19222.
8. biodegradable plastics: ecotoxicity comparison between polyvinylchloride and Mater-Bi® micro-debris in a freshwater biological model. *Science of the Total Environment*, 720: 137602.
9. Briassoulis, D., Pikasi, A. and Hiskakis, M., 2021. Recirculation potential of post-consumer/industrial bio-based plastics through mechanical recycling-Techno-economic sustainability criteria and indicators. *Polymer Degradation and Stability*, 183: p.109217.
10. Chen, X., & Yan, N., 2020. A brief overview of renewable plastics. *Materials Today Sustainability*, 7: p.100031.
11. doped by Ni/ZnO nanohybrid for food packaging applications. *Journal of Materials Research and Technology*, 19: pp.3421-3432.
12. Gurunathan, T., Mohanty, S., & Nayak, S. K., 2015. A review of the recent developments in biocomposites based on natural fibres and their application perspectives. *Composites Part A: Applied Science and Manufacturing*, 77: pp.1-25.
13. Hassan Basri, H., Talib, R.A., Sukor, R., Othman, S.H. and Ariffin, H., 2020. Effect of synthesis temperature on the size of ZnO nanoparticles derived from pineapple peel extract and antibacterial activity of ZnO-starch nanocomposite films. *Nanomaterials*, 10(6): p.1061.
14. Hu, X., Jia, X., Zhi, C., Jin, Z. and Miao, M., 2019. Improving the properties of starch-based antimicrobial composite films using ZnO-chitosan nanoparticles. *Carbohydrate polymers*, 210: pp.204-209.
15. Hussein, J., El-Naggar, M.E., Fouda, M.M., Morsy, O.M., Ajarem, J.S., Almalki, A.M., Allam, A.A. and Mekawi, E.M., 2020. The efficiency of blackberry loaded AgNPs, AuNPs and Ag@ AuNPs mediated pectin in the treatment of cisplatin-induced cardiotoxicity in experimental rats. *International Journal of Biological Macromolecules*, 159: pp1084-1093
16. Iqbal, M.J. and Iqbal, S., 2013. Synthesis of stable and highly luminescent beryllium and magnesium doped ZnS quantum dots suitable for design of photonic and sensor material. *Journal of luminescence*, 134: pp.739-746.
17. Iqbal, S., Bahadur, A., Saeed, A., Zhou, K., Shoaib, M. and Waqas, M., 2017. Electrochemical performance of 2D polyaniline anchored CuS/Graphene nano-active composite as anode material for lithium-ion battery. *Journal of colloid and interface science*, 502: pp.16-23.
18. Jadhav, A. C., Pandit, P., Gayatri, T. N., Chavan, P. P., & Jadhav, N. C., 2019. Production of green composites from various sustainable raw materials. *Green Composites: Sustainable Raw Materials*: pp.1-24.
19. Jang, J., & Lee, D. K., 2003. Plasticizer effect on the melting and crystallization behavior of polyvinyl alcohol. *Polymer*, 44(26): pp.8139-8146.
20. Kabir, E., Kaur, R., Lee, J., Kim, K. H., & Kwon, E. E., 2020. Prospects of biopolymer technology as an alternative option for non-degradable plastics and sustainable management of plastic wastes. *Journal of Cleaner Production*, 258: p.120536.
21. Lian, R., Cao, J., Jiang, X. and Rogachev, A.V., 2021. Physicochemical, antibacterial properties and cytocompatibility of starch/chitosan films incorporated with zinc oxide nanoparticles. *Materials Today Communications*, 27: p.102265.
22. Lopez, C. G., Rogers, S. E., Colby, R. H., Graham, P., & Cabral, J. T., 2015. Structure of sodium carboxymethyl cellulose aqueous solutions: A SANS and rheology study. *Journal of Polymer Science Part B: Polymer Physics*, 53(7): pp.492-501.
23. Magni, S., Bonasoro, F., Della Torre, C., Parenti, C. C., Maggioni, D., & Binelli, A., 2020. Plastics and



24. Mhatre, A. M., Raja, A. S. M., Saxena, S., & Patil, P. G., 2019. Environmentally benign and sustainable green composites: current developments and challenges. *Green Composites: Sustainable Raw Materials*: pp.53-90.
25. Mondal, A., Chouke, P.B., Sonkusre, V., Lambat, T., Abdala, A.A., Mondal, S. and Chaudhary, R.G., 2020. Ni-doped ZnO nanocrystalline material for electrocatalytic oxygen reduction reaction. *Materials Today: Proceedings*, 29: pp.715-719.
26. N. F., Alsaedi, M. A., & Aman, A., 2014. Dielectric properties of polyvinyl chloride with wollastonite filler for the application of high-voltage outdoor insulation material. *Arabian Journal for Science and Engineering*, 39: pp.3999-4012.
27. Saba, N., Jawaid, M., & Asim, M., 2019. Nanocomposites with nanofibers and fillers from renewable resources. In *Green composites for automotive applications*: (pp. 145-170). Woodhead Publishing.
28. Saemi, R., Taghavi, E., Jafarizadeh-Malmiri, H. and Anarjan, N., 2021. Fabrication of green ZnO nanoparticles using walnut leaf extract to develop an antibacterial film based on polyethylene–starch–ZnO NPs. *Green Processing and Synthesis*, 10(1): pp.112-124.
29. Saikia, A., Hazarika, D., & Karak, N., 2019. Tough and biodegradable thermosets derived by blending of renewable resource based hyperbranched epoxy and hyperbranched polyester. *Polymer Degradation and Stability*, 159: pp.15-22.
30. Shabana, S., Prasansha, R., Kalinina, I., Potoroko, I., Bagale, U., & Shirish, S. H., 2019. Ultrasound assisted acid hydrolyzed structure modification and loading of antioxidants on potato starch NPs. *Ultrasonics sonochemistry*, 51: pp.444-450.
31. Shafqat, A., Tahir, A., Mahmood, A., Tabinda, A.B., Yasar, A. and Pugazhendhi, A., 2020. A review on environmental significance carbon foot prints of starch based bio-plastic: A substitute of conventional plastics. *Biocatalysis and agricultural biotechnology*, 27: p.101540.
32. Shen, D., Li, X., Ma, C., Zhou, Y., Sun, L., Yin, S., Huo, P. and Wang, H., 2020. Synthesized Z-scheme photocatalyst ZnO/gC₃N₄ for enhanced photocatalytic reduction of CO₂. *New Journal of Chemistry*, 44(38): pp.16390-16399.
33. Shen, M., Song, B., Zeng, G., Zhang, Y., Huang, W., Wen, X., & Tang, W, 2020. Are biodegradable plastics a promising solution to solve the global plastic pollution?. *Environmental Pollution*, 263: p. 114469.
34. Sintim, H.Y., Bary, A.I., Hayes, D.G., Wadsworth, L.C., Anunciado, M.B., English, M.E., Bandopadhyay, S., Schaeffer, S.M., DeBruyn, J.M., Miles, C.A. and Reganold, J.P., 2020. In situ degradation of biodegradable plastic mulch films in compost and agricultural soils. *Science of the total environment*, 727: p.138668.
35. Tran, N. H. A., Hund, R. D., Kemnitzer, J., Schwarzer, J., & Cherif, C., 2019. An eco-friendly post-drawing process for splitting bicomponent filaments. *Materials Letters*, 237: pp. 258-261.
36. Waqas, M., Iqbal, S., Bahadur, A., Saeed, A., Raheel, M. and Javed, M., 2017. Designing of a spatially separated hetero-junction pseudobrookite (Fe₂TiO₅-TiO₂) yolk-shell hollow spheres as efficient photocatalyst for water oxidation reaction. *Applied Catalysis B: Environmental*, 219: pp.30-35.
37. Yaacob, M. M., Kamaruddin, N., Mazlan, N. A., Noramat,
38. Zare, Y. and Rhee, K.Y., 2019. Expression of normal stress difference and relaxation modulus for ternary nanocomposites containing biodegradable polymers and carbon nanotubes by storage and loss modulus data. *Composites Part B: Engineering*, 158: pp.162-168.

ACKNOWLEDGMENT



The authors thank to all of the co-authors who took part in this study on their own free will, as well as the administrators of the institution who authorised research.

CONFLICT OF INTEREST

There is no conflict of interest, according to the authors.